Effect of Substrate Surface on Dewetting Behavior and Chain Orientation of Semicrystalline Block Copolymer Thin Films

Guo-Dong Liang, Jun-Ting Xu,* and Zhi-Qiang Fan

Key Laboratory of Macromolecular Synthesis and Functionalization, Department of Polymer Science & Engineering, Zhejiang University, Hangzhou 310027, China

Shao-Min Mai and Anthony J. Ryan

Department of Chemistry, The University of Sheffield, Sheffield S3 7HF, U.K.

Received: June 27, 2006; In Final Form: September 20, 2006

Three symmetrical semicrystalline oxyethylene/oxybutylene block copolymers (E_mB_n) were spin-coated on different substrates including silicon, hydrophobically modified silicon, and mica. The effects of surface property on the dewetting behavior of E_mB_n thin films and the chain orientation of the crystalline block were investigated with atomic force microscopy and grazing incidence X-ray diffraction . The E_mB_n thin films on silicon exhibit an autophobic dewetting behavior, while ordinary dewetting occurs for the thin films on modified silicon. It was observed that the stems of the E crystals in the first half-polymer layer contacting the mica surface were parallel to the surface, in contrast to the perpendicular chain orientation of the other polymer layers and of the first half-polymer layer on silicon. This is attributed to the strong interaction between the E block and mica, verified by infrared spectra.

Introduction

The thin film morphology of block copolymers has attracted increasing interest because of their scientific importance and potential uses in a range of applications.[1−3] The morphology of block polymer thin films is affected by various factors such as polymer structure, substrate surface properties, preparation conditions, and thermal history, among which the substrate surface is one of the most important factors for a given polymer. For example, when the substrate surface preferentially absorbs one segment of a symmetrical block copolymer, a lamellar phase structure parallel to the surface is usually formed, while a lamellar phase structure perpendicular to the surface may be formed when the surface is neutral to both blocks.[1] The substrate surface property also affects the dewetting behavior of block copolymers. An autophobic dewetting phenomenon, which refers to dewetting between molecules with the same chemical composition, sometimes is observed in block copolymers.[4−8] Generally, it is believed that autophobic dewetting is driven by entropy,[9−12] meaning that the conformation of the first block copolymer layer contacting the substrate surface is different from that of the other polymer layers. Green et al.[13,14] observed that the substrate surface can induce microphase separation above the order−disorder transition temperature (T_{ODT}) in the bulk due to the interaction between the block copolymer and substrate. However, below T_{ODT} the subtle change in the conformation of the block copolymers on the substrate is difficult to characterize and thus the interaction between the block copolymer and substrate cannot be determined.

In this paper, we will study the thin film morphology of a set of semicrystalline E_mB_n block copolymers on various substrates. There are two situations when there is a favorable interaction between the substrate surface and the crystalline E block. The first occurs when the stems of the crystalline block are perpendicular to the substrate surface. Since in semicrystalline block copolymers the conformation of the amorphous block and chain folding of the crystalline block affect each other and the long period is determined by the balance of these two factors,[15−18] it is expected that larger E block chain folds may be induced by the substrate and result in a smaller long period being observed. In block copolymer thin films, the thickness of polymer layers is usually xL_0 for symmetrical wetting or $(x + 1/2)L_0$ for asymmetrical wetting (where L_0 is the long period of block copolymer in bulk and x is an integer).[19] When the thickness of the thin film does not meet this condition, films with $x > 1$ form rough surfaces with holes and islands, whereas in films thinner than $x = 1$, dewetting will take place. As a result, the change in the long period of the semicrystalline block copolymer induced by the substrate surface can be reflected by the thickness of the thin film. The second situation occurs when the crystal stems of the E block are induced to lie down parallel to the substrate surface due to a strong interaction between the substrate and the E block. In this situation, it is expected that different chain orientations of the crystalline E block can be observed for different substrates, even for different polymer layers in the same film.

Experimental Section

Materials. The synthesis and characterization of oxyethylene/oxybutylene block copolymers, $E_{76}B_{38}$, $E_{114}B_{56}$, and $E_{155}B_{76}$ (where E and B denote oxyethylene and oxybutylene units, respectively, which are denoted as E_mB_n and the subscripts refer to the average degree of polymerization) have been described elsewhere.[20−22] All the block copolymers have narrow molecular weight distributions ($M_w/M_n < 1.05$) as measured by gel permeation chromagotraphy and have a lamellar phase morphol-

* Corresponding author. E-mail: xujt@zju.edu.cn. Fax: +86-571-87952400.

10.1021/jp064008s CCC: $33.50
Published on Web 11/07/2006

TABLE 1: Molecular Characterization of E_mB_n Diblock Copolymers

copolymers	ϕ_E[a] (solid state)	w_E[b] (solid state)	long period in the bulk L_0 (nm)	T_c (°C)[c]	$N\cdot\chi$[d]
$E_{76}B_{38}$	0.49	0.55	16.7	35	19.9
$E_{114}B_{56}$	0.50	0.55	19.8	38	29.7
$E_{155}B_{76}$	0.50	0.56	22.0	40	40.4

[a] $\phi_E = m/[m + (72/44)(1.23/0.97)n]$; ϕ_E is the volume fraction of the E block, 1.23 g/cm^3 being the density of E in the crystalline state and 0.97 g/cm^3 the density of B in the liquid state, both at 20 °C. [b] $w_E = m/[m + (72/44)n]$; w_E is the weight fraction of the E block. [c] T_c: at cooling rate of 10 °C/min. [d] χ: calculated for E_mB_n diblock copolymer bulk at 20 °C.

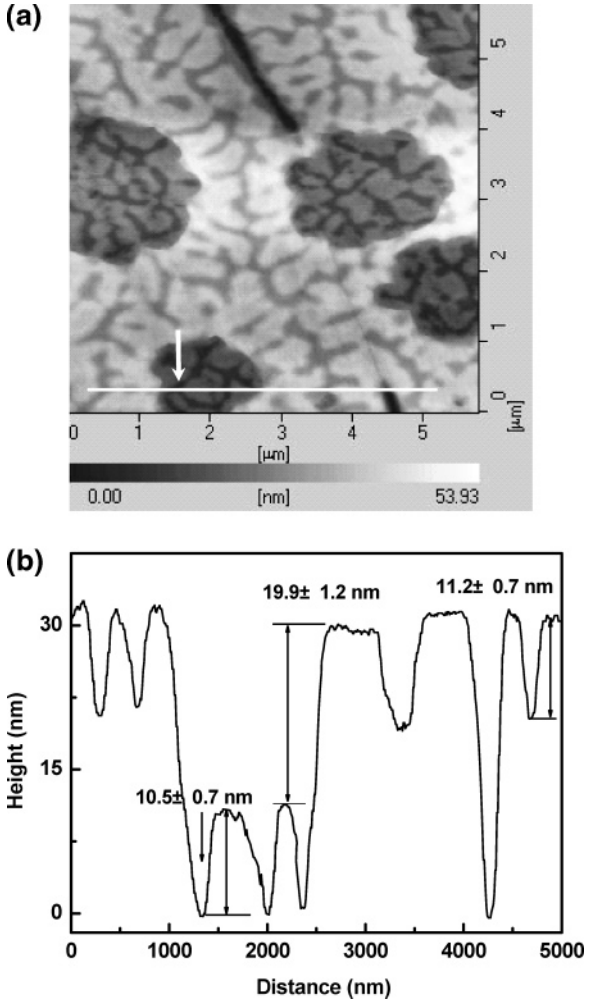

Figure 1. AFM height image (a) and cross-sectional profile (b) of nascent $E_{155}B_{76}$ thin film on silicon.

ogy in both the solid and liquid bulk phases. The molecular characteristics of the block copolymers are summarized in Table 1. The single-crystal silicon wafers (p-type, 6 in. in diameter) were supplied by the Shanghai Institute of Ceramics, China. They were cut into strips of about 10 mm × 10 mm and then treated with "piranha" solution, a mixture of 70 vol % concentrated sulfuric acid and 30 vol % hydrogen peroxide, for about 30 min at 60 °C to generate a clean, hydrophilic oxide surface. The substrate was then rinsed with a large volume of distilled water and dried in a vacuum oven at 80 °C for 8 h. When mica was used as substrate, the first several layers on the top of the mica were stripped and the block copolymers were spin-coated on the clean and fresh mica surface.

Modification of Silicon Surface. The vapor-phase method was chosen to modify silicon wafers, which can induce the formation of a monolayer of silane film on a solid surface bearing hydroxyl groups. Some silicon chips of about 10 mm × 10 mm were attached to plastic plates, and then about 5 mL of trimethylchlorosilane wasdeposited into a 50 mL plastic jar. The plastic plates were placed on the jar, mounted so that the fresh surface was facing the silane liquid. After placement of the jar into a vacuum desiccator, the desiccator was evacuated to 10 Torr. The substrates were then allowed to react with the silane vapor for 5 h at room temperature. After being ultrasonically cleaned with dry toluene and then ethanol for 10 min, respectively, the substrates were cured at 120 °C for 3 h in an oven under ambient pressure. The water contact angle of modified silicon increased from 84.8° to 116.0° with time, whereas the water contact angle of the initial hydrophilic silicon substrate decreased from 28.4° to <5° with time.

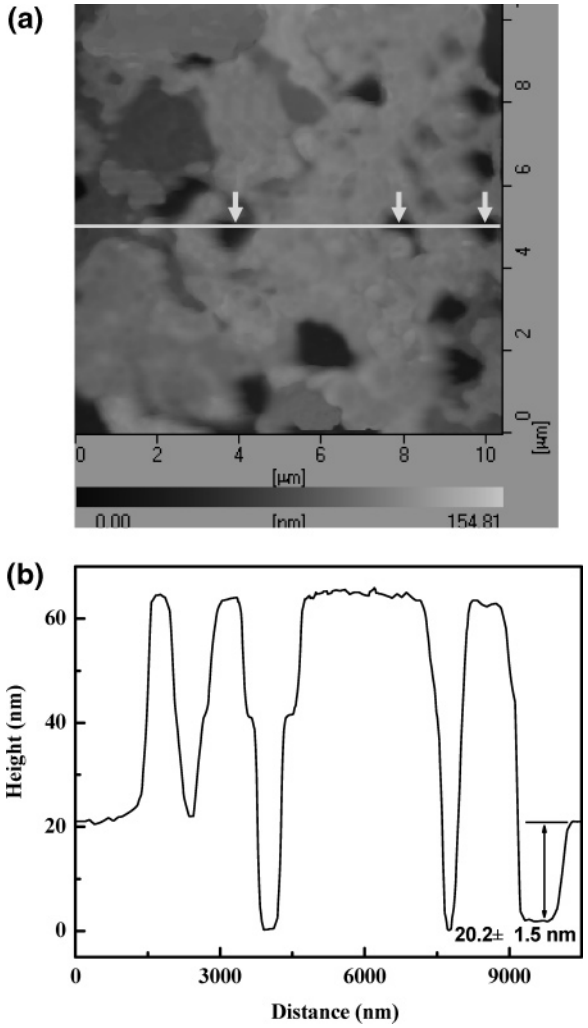

Figure 2. AFM height image (a) and cross-sectional profile (b) of nascent $E_{155}B_{76}$ thin film on modified silicon.

Preparation of Diblock Copolymer Thin Films. Block copolymer thin films were prepared by spin-coating E_mB_n/dichloromethane solutions on various substrates. The concentration of the solution was 0.5 w/v for silicon and modified silicon and 1.0 w/v for mica. Annealing of the diblock copolymer thin films was conducted at 35 °C for 30 h in a vacuum system (10 Torr). This annealing temperature is near the crystallization temperature of the E block. We chose 35 °C as the annealing temperature for the following reasons: (1) At this temperature, the thin film is crystallized and dewetting behavior associated with crystallization can be observed. (2) Since parts of the E block are already crystalline, the E block crystals can act as

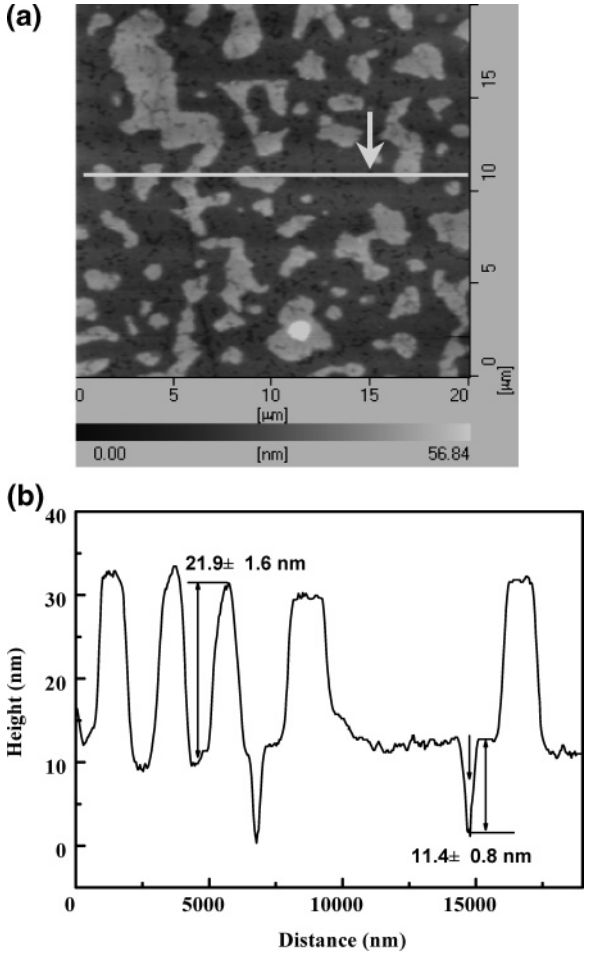

Figure 3. AFM height image (a) and cross-sectional profile (b) of annealed $E_{155}B_{76}$ thin film on silicon.

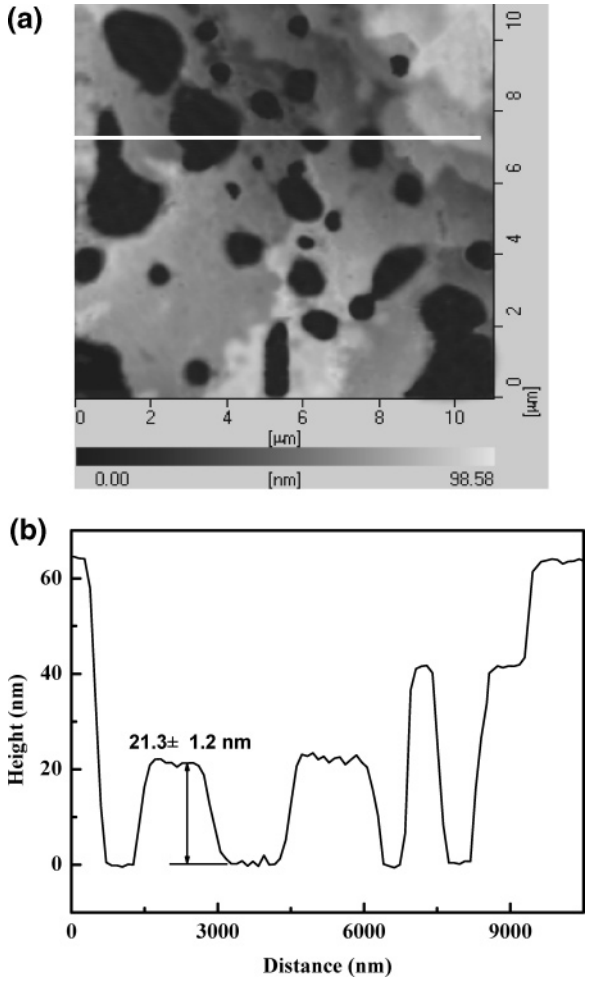

Figure 4. AFM height image (a) and cross-sectional profile (b) of annealed $E_{155}B_{76}$ thin film on modified silicon.

nuclei during secondary crystallization due to annealing. As a result, the nucleation from the substrate can be ignored. (3) At lower annealing temperatures, the evolution of the morphology is slow and this facilitates off-line atomic force microscopy (AFM) observations and other experiments. On the other hand, a higher annealing temperature leads to a faster morphological evolution and so it is not easy to get high quality AFM images. However, it should also be noted that although the annealing temperature is only 35 °C (lower than the melting temperature of the E crystals), equilibrated morphology can be reached such that no further morphological change can be observed at longer annealing times.

Atomic Force Microscopy. The thin film morphology of the E_mB_n block copolymers was investigated by atomic force microscopy (SPA 300HV/SPI3800N Probe Station, Seiko instruments Inc., Japan) in tapping mode. A silicon microcantilever with a spring constant 16 of N/m and a resonance frequency of about 138 kHz was used. The scan rate for optimal AFM image quality ranged from 0.5 to 2.0 Hz. The set-point ratio, the ratio between the set-point amplitude and the free vibration amplitude (the lowest amplitude when tip and sample are not in contact), was chosen to be about 0.8. Parameters characterizing features of the thin film such as lamellar thickness were obtained directly from the cross-sectional profiles. To ensure the repeatability of the data, cross-sectional profiles from different areas were necessary. At least 10 values were obtained for each parameter.

Grazing Incidence X-ray Diffraction (GIXRD). Grazing incidence techniques were carried out to investigate the crystal structure of the diblock copolymer thin film at room temperature. A BEDE D1 high-resolution X-ray diffractometerequipped with a Cu Kα radiation source was used. The diffracted beam is in the plane defined by the incidence beam and the surface normal. This geometry is sensitive to the structure parallel to the surface. Different grazing incidence angles ranging from 0.2° to 0.8° were tested. The XRD curves were scanned in the 2θ range of 3.0−30°.

Fourier Transformation Infrared (FTIR) Spectroscopy. FTIR spectroscopy was carried out on a BrukerVector 22 spectrometer. The poly(ethylene oxide) (PEO) homopolymer with $M_n = 2\,000$ was blended with mica particles. The diameter of the mica particles was about 50 μm.

Results and Discussion

Dewetting Behavior. Figures 1 and 2 show the AFM images of nascent (as-spun) $E_{155}B_{76}$ thin films on silicon and modified silicon, respectively. Both thin films are composed of multiple polymer layers with irregular holes. As reported previously,[23] there is a half-polymer layer with thickness $L \approx (1/2)L_0$ on the silicon due to preferential absorption of the E block by the silicon forming an asymmetrical film structure. In contrast, a symmetrical thin-film structure is obtained on the modified silicon surface because the hydrophobic B block tends to be located at both the modified silicon surface and the polymer/air interface. The nascent thin films of $E_{76}B_{38}$ and $E_{114}B_{56}$ exhibit similar morphology.

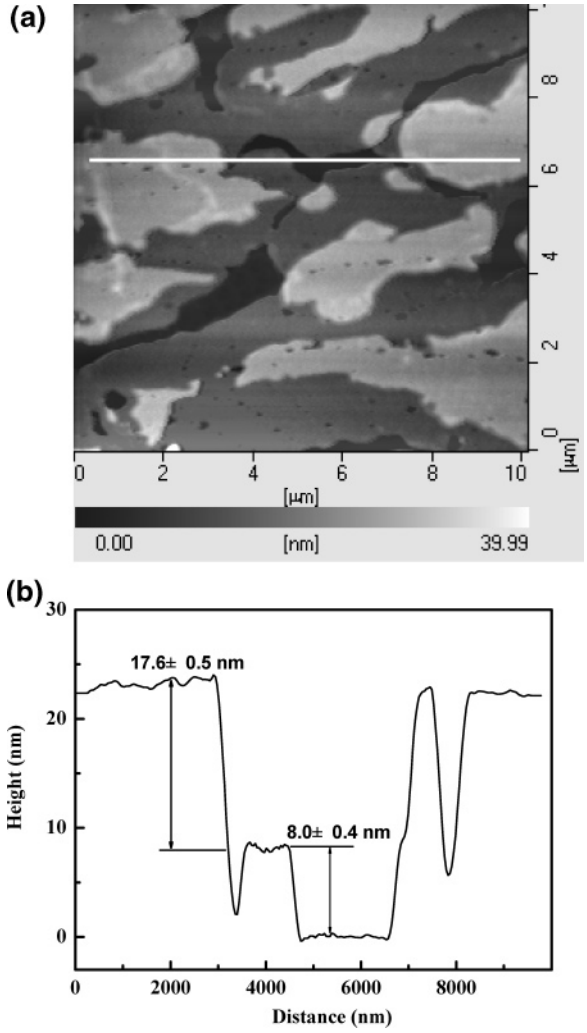

Figure 5. AFM height image (a) and cross-sectional profile (b) of annealed $E_{76}B_{38}$ thin film on mica.

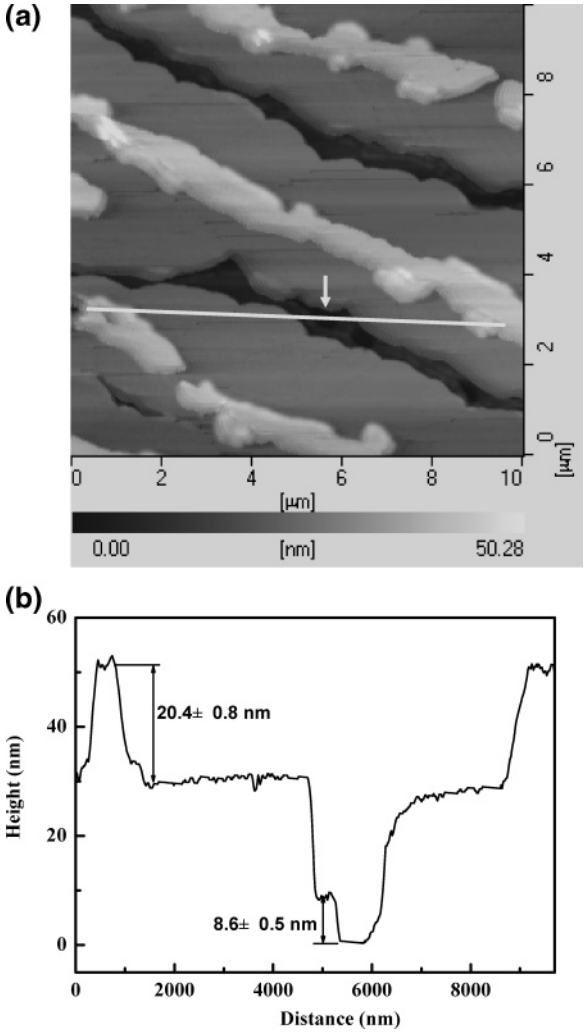

Figure 6. AFM height image (a) and cross-sectional profile (b) of annealed $E_{114}B_{56}$ thin film on mica.

The AFM images of annealed $E_{155}B_{76}$ thin films on silicon and modified silicon are shown in Figures 3 and 4, respectively. One can see that the dewetting behaviors of $E_{155}B_{76}$ on these two surfaces are quite different. On silicon, the first half-polymer layer contacting the substrate surface spreads over the silicon surface during annealing and the size of the holes left on this half-polymer layer become much smaller, indicating good wetting. On the top of this half-polymer layer, the block copolymers dewet and an island pattern forms. Although only polymer islands are formed on the upper layer in the final morphology, retraction of the polymer and development of holes in the upper layer are indeed observed during dewetting (see Figure S1 in the Supporting Information). This is a typical autophobic phenomenon; i.e., dewetting takes place for $E_{155}B_{76}$ on its own polymer layer. In contrast, on the modified silicon surface, holes of larger size developed during annealing and the naked substrate surface was gradually exposed, indicating an ordinary dewetting phenomenon. The dewetting behaviors of $E_{76}B_{38}$ and $E_{114}B_{56}$ thin films on silicon and modified silicon are similar to those of $E_{155}B_{76}$. This result shows that the dewetting behavior of semicrystalline E_mB_n thin films strongly depends on the surface properties of the substrate.

It is generally believed that the autophobic dewetting phenomenon is due to the different conformations of the first polymer layer contacting the substrate surface and other polymer layers. In thin films of semicrystalline block copolymers, such a difference in conformation should be reflected by a change of thin film thickness, since the chain folding of the crystalline block and the conformation of the amorphous block are related to the long period and film thickness. However, when the thickness of the first half-polymer layer on silicon is compared with the $(1/2)L_0$ in the bulk and the half thickness of other polymer layers or when the thickness of the first half-polymer layer on silicon is compared with the half thickness of the first polymer layer on modified silicon, no significant difference is observed. This shows that the change in E_mB_n conformation induced by the silicon surface is very small and cannot be detected by AFM due to the roughness of the thin film.

Effect of Substrate on Chain Orientation. To enhance the interaction between E_mB_n and the substrate surface, we chose a mica substrate and studied the thin film morphology of E_mB_n on mica. It is well-known that mica is a layered silicate and contains different kinds of cations, especially abundant K^+.[24−26] The oxygen atoms in the E block may coordinate with these cations,[27] causing a strong interaction between the surface of mica and the E block. The AFM images of E_mB_n block copolymers thin films after annealing at 35 °C for 30 h are shown in Figures 5−7, respectively. The thin films are composed of multiple layers of polymer parallel to the substrate surface as well. On the top surface of the mica is a half layer of polymer, since the E block is absorbed on the hydrophilic mica surface, whereas the hydrophobic B block is located at the polymer/air interface.

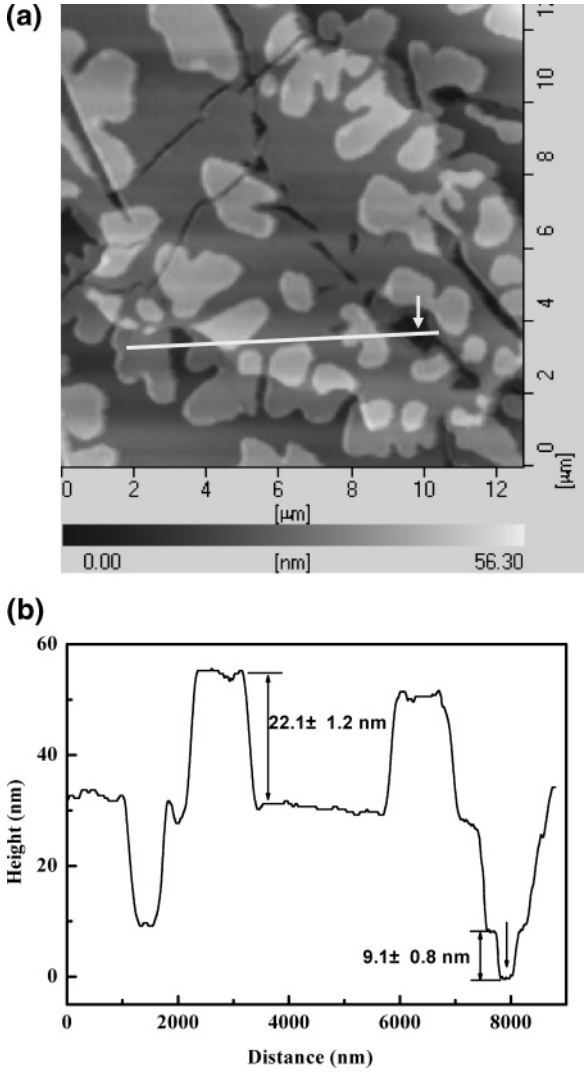

Figure 7. AFM height image (a) and cross-sectional profile (b) of annealed $E_{155}B_{76}$ thin film on mica.

Before the discussion of the effect of substrate on chain conformation in semicrystalline block copolymers, the chain orientation of the crystalline block must be determined. We used grazing incidence X-ray diffraction to probe the chain orientation of the crystal stems. According to the geometry of GIXRD, only the reflections parallel to the substrate surface can be detected.[28−30] The penetration depth of the X-rays into the thin films is dependent on the incidence angle (a_i). The larger the incidence angle, the deeper the penetration of the X-rays. Various incidence angles ranging from 0.2° to 0.8° were tested so that chain orientation in different polymer layers could be probed. The GIXRD patterns of the annealed E_mB_n thin films on mica at $a_i = 0.6°$ and $a_i = 0.2°$ are shown in Figures 8 and 9, respectively. It is found that at larger incidence angle ($a_i = 0.6°$), the (120) reflection of the PEO crystals can be observed for the thin films of all three block copolymers. However, such a peak cannot be observed at a smaller incidence angle ($a_i = 0.2°$). It should be noted that the diffractions from mica still appear at the incidence angle of 0.2°, which is due to the incomplete coverage of the mica surface by the E_mB_n block copolymers. The GIXRD results imply that the crystal stems of the E block in different layers have different chain orientations. In the half-polymer layer near the mica surface, the stems of the E crystals are parallel to the surface, while in the upper polymer layers the stems of the E crystals are perpendicular to the surface. This

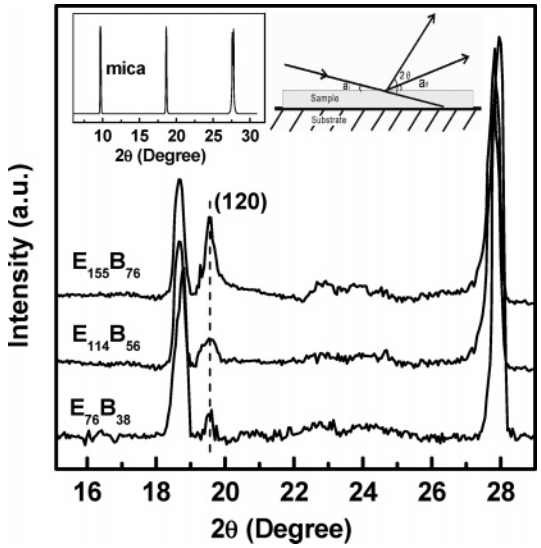

Figure 8. GIXRD patterns of annealed E_mB_n thin films on mica at an incidence angle of 0.6°. The insets are the GIXRD pattern of mica and the geometry of GIXRD.

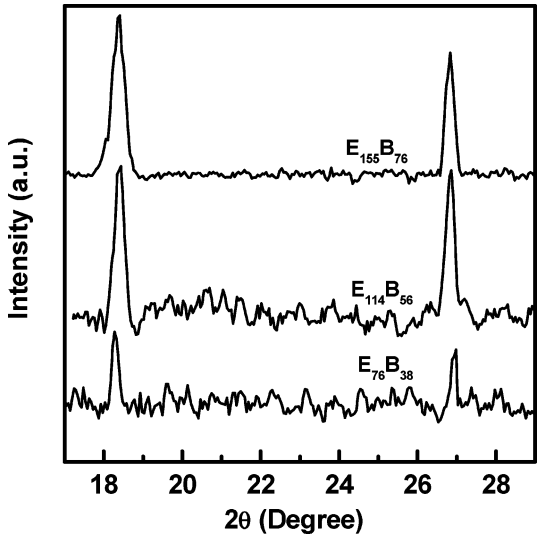

Figure 9. GIXRD patterns of annealed E_mB_n thin films on mica at an incidence angle of 0.2°.

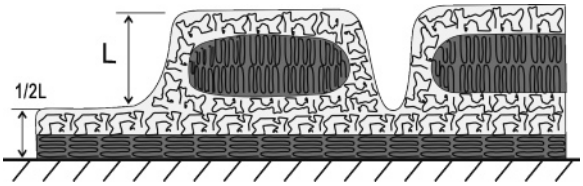

Figure 10. Schematic structure for E_mB_n thin films on mica.

conclusion is further confirmed by the GIXRD patterns of the annealed half-layered thin films of E_mB_n on mica, which were prepared by the spin-coating of a 0.5% E_mB_n solution. For the half-layered thin films of E_mB_n on mica, even at the incidence angle $a_i = 0.2°$, the (120) reflection of the E crystals is observed (see Figure S3 in the supporting information). The morphology of the E_mB_n block copolymers is schematically shown in Figure 10. The chain orientation of the first half layer contacting mica surface is also different from that of the first half layer on the silicon surface,[23] though both substrates are hydrophilic. We notice that even at larger incidence angles ($a_i = 0.6°$), the (120) reflection was not observed in the GIXRD patterns of the thin films of $E_{76}B_{38}$, $E_{114}B_{56}$, and $E_{155}B_{76}$ on silicon.[23] The different

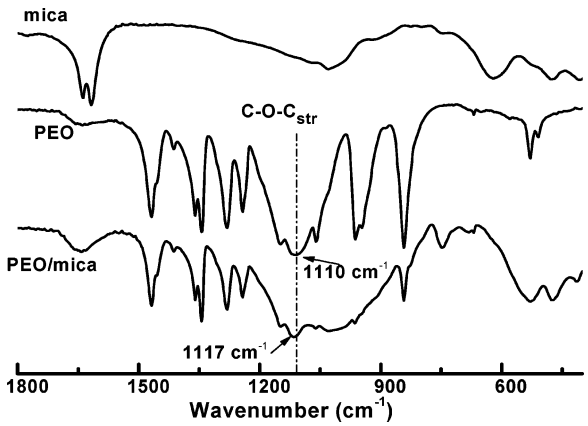

Figure 11. FTIR spectra of PEO homopolymer, mica, and a PEO/mica blend.

chain orientation of the first half-polymer layer on mica from that in other polymer layers and from that on silicon clearly reveals that it is induced by the strong interaction between the E block and mica. To verify the interaction between mica and the E block, we blended PEO homopolymer with mica particles having a diameter of about 50 μm. The FTIR spectra of neat PEO, mica, and a PEO/mica blend are shown in Figure 11. It is found that the stretching band of the C−O−C backbone in PEO shifts from 1110 cm^{-1} for neat PEO to 1117 cm^{-1} for the PEO/mica blend, which can be ascribed to the interaction between the PEO and mica. Such an interaction may induce the E block in the first polymer layer contacting the mica surface to lie down on the surface and to adopt a chain orientation parallel to the surface.

Conclusions

The substrate surface has been shown to have a considerable influence on the wetting behavior of E_mB_n block copolymers. Autophobic dewetting is observed for E_mB_n thin film on silicon, while ordinary dewetting occurs on modified silicon. There is a strong interaction between the E block and mica, which is confirmed by IR spectra. Such a favorable interaction can induce a change in chain orientation of the crystalline block. The GIXRD results show that the stems of the E crystals in the first half-polymer layer contacting mica surface are parallel to the surface, as opposed to the perpendicular chain orientation in the other polymer layers and in the first half-polymer layer on silicon.

Acknowledgment. This research was supported by ICI and the National Natural Science Foundation of China (20374046), the Excellent Young Teachers Program, and the New Century Supporting Program for the Talents by the Chinese Ministry of Education. The authors also would like to thank Professor Stephen Z. D. Cheng at the University of Akron for helpful discussion.

Supporting Information Available: Morphological change of the $E_{155}B_{76}$ thin film on silicon during annealing, AFM height image of half-layered $E_{76}B_{38}$ thin film on mica, and GIXRD patterns of half-layered E_mB_n thin films on mica. This material is available free of charge via the Internet at http://pubs.acs.org.

References and Notes

(1) Fasolka, M. J.; Mayes, A. M. *Annu. Rev. Mater. Res.* **2001**, *31*, 323.

(2) Granick, S.; Kumar, S. K.; Amis, E. J.; Antonietti, M.; Balazs, A. C.; Chakraborty, A. K.; Grest, G. S.; Hawker, C.; Janmey, P.; Kramer, E. J.; Nuzzo, R.; Russell, T. P.; Safinya, C. R. *J. Polym. Sci., Part B: Polym. Phys.* **2003**, *41*, 2755.

(3) Segalman, R. A. *Mater. Sci. Eng., R:* **2005**, *48*, 191.

(4) Hamley, I. W.; Hiscutt, E. L.; Yang, Y. W.; Booth, C. *J. Colloid Interface Sci.* **1999**, *209*, 255.

(5) Fukunaga, K.; Elbs, H.; Magerle, R.; Krausch, G. *Macromolecules* **2000**, *33*, 947.

(6) Fukunaga, K.; Hashimoto, T.; Elbs, H.; Krausch, G. *Macromolecules* **2002**, *35*, 4406.

(7) Lee, S. H.; Kang, H. M.; Kim, Y. S.; Char, K. *Macromolecules* **2003**, *36*, 4907.

(8) Zhu, J. T.; Zhao, J. C.; Liao, Y. G.; Jiang, W. *J. Polym. Sci., Part B: Polym. Phys.* **2005**, *43*, 2874.

(9) Liu, Y.; Rafailovich, M. H.; Sokolov, J.; Schwarz, S. A.; Zhong, X.; Eisenberg, A.; Kramer, E. J.; Sauer, B. B. *Phys. Rev. Lett.* **1994**, *73*, 440.

(10) Shull, K. R. *Faraday Discuss.* **1994**, *98*, 203.

(11) Ferreira, P. G.; Ajdari, A.; Leibler, L. *Macromolecules* **1998**, *31*, 3994.

(12) Reiter, G.; Khanna, R. *Phys. Rev. Lett.* **2000**, *85*, 5599.

(13) Limary, R.; Green, P. F. *Macromolecules* **1999**, *32*, 8167.

(14) Limary, R.; Green, P. F. *Langmuir* **1999**, *15*, 5617.

(15) DiMarzio, E. A.; Guttman, C. M.; Hoffmann, J. D. *Macromolecules* **1980**, *13*, 1194.

(16) Whitmore, M. D.; Noolandi, J. *Macromolecules* **1988**, *21*, 1482.

(17) Vilgis, T.; Halperin, A. *Macromolecules* **1991**, *24*, 2090.

(18) Ryan, A. J.; Fairclough, J. P. A.; Hamley, I. W.; Mai, S. M.; Booth, C. *Macromolecules* **1997**, *30*, 1723.

(19) Green, P. F. *J. Polym. Sci., Part B: Polym. Phys.* **2003**, *41*, 2219.

(20) Mai, S. M.; Fairclough, J. P. A.; Viras, K.; Gorry, P. A.; Hamley, I. W.; Ryan, A. J.; Booth, C. *Macromolecules* **1997**, *30*, 8392.

(21) Mai, S. M.; Fairclough, J. P. A.; Terrill, N. J.; Turner, S. C.; Hamley, I. W.; Matsen, M. W.; Ryan, A. J.; Booth, C. *Macromolecules* **1998**, *31*, 8110.

(22) Ryan, A. J.; Mai, S. M.; Fairclough, J. P. A.; Hamley, I. W.; Booth, C. *Phys. Chem. Chem. Phys.* **2001**, *3*, 2961.

(23) Liang, G. D.; Xu, J. T.; Fan, Z. Q.; Mai, S. M.; Ryan, A. J. *Macromolecules* **2006**, *39*, 5471.

(24) Geke, M. O.; Shelden, R. A.; Caseri, W. R.; Suter, U. W. *J. Colloid Interface Sci.* **1997**, *189*, 283.

(25) Surin, M.; Marsitzky, D.; Grimsdale, A. C.; Mullen, K.; Lazzaroni, R.; Leclere, P. *Adv. Funct. Mater.* **2004**, *14*, 708.

(26) Chai, L.; Klein, J. *J. Am. Chem. Soc.* **2005**, *127*, 1104.

(27) Yu, K.; Eisenberg, A. *Macromolecules* **1998**, *31*, 3509.

(28) Durell, M.; Macdonald, J. E.; Trolley, D.; Wehrum, A.; Jukes, P. C.; Jones, R. A. L.; Walker, C. J.; Brown, S. *Europhys. Lett.* **2002**, *58*, 844.

(29) Murthy, N. S.; Bednarczyk, C.; Minor, H. *Polymer* **2000**, *41*, 277.

(30) Lee, B.; Park, I.; Yoon, J.; Park, S.; Kim, J.; Kim, K. W.; Chang, T.; Ree, M. *Macromolecules* **2005**, *38*, 4311.